Bull. Chem. Soc. Ethiop. **2022**, 36(3), 555-569.
DOI: https://dx.doi.org/10.4314/bcse.v36i3.6

ISSN 1011-3924
Printed in Ethiopia
Online ISSN 1726-801X

$Al_2O_3/Fe_3O_4/ZrO_2$ TERNARY OXIDE SORBENT: SYNTHESIS, CHARACTERIZATION AND SORPTION BEHAVIOR TO FLUORIDE AND PHOSPHATE IONS FROM AQUEOUS SOLUTION

Wubishet Legese, Abi M. Taddesse and Endale Teju*

Department of Chemistry, College of Natural and Computational Sciences, Haramaya University, Haramaya, Ethiopia. P.O. Box, 138, Dire Dawa, Ethiopia

Received April 27, 2022; Revised June 18, 2022; Accepted June 18, 2022

ABSTRACT. Excess quantities of fluoride and phosphate in water bodies can lead to fluorosis and eutrophication problems, respectively. In search of a promising adsorbent targeting these ions, $Fe_3O_4/Al_2O_3/ZrO_2$ ternary oxide was synthesized via co-precipitation method and characterized by X-ray diffraction (XRD), Fourier transform-infrared (FTIR) and Brunauer-Emmer-Teller (BET). Its specific surface area was found to be 205 m^2/g. The effects of solution pH, adsorbent dose, contact time, agitation speed and initial fluoride and phosphate concentrations were also investigated and the optimum values were 4, 0.5 g, 12 h, 100 rpm and 20 mg/L, respectively, for fluoride and 5, 0.1 g, 8 h, 100 rpm and 10 mg/L, respectively, for phosphate. Fluoride and phosphate adsorptions fitted well with Freundlich and Langmuir isotherm models, respectively and their kinetic data correlated well with the pseudo-second order model. Desorbability study revealed that maximum desorption was achieved at pH 12. Thermodynamics study on the other hand showed that adsorption of fluoride was nonspontaneous and endothermic whereas that of phosphate was spontaneous and exothermic. Application on real water sample decreased the concentration of fluoride from 4.92 to 1.97 mg/L in ground water and phosphate from 1.7 to 0.35 mg/L lake water showing its potential as a promising adsorbent.

KEY WORDS: Adsorption, Fluoride, Phosphate, Ternary oxide sorbent, Isotherm models

INTRODUCTION

Quality of water resources is deteriorating continuously due to geometrical growth of population, industrialization, civilization, domestic and agricultural activities and other geological and environmental changes [1, 2]. In this regard, water pollution has become a serious issue in the present scenario, affecting all living creatures, household, recreation, fishing, transportation, and other commercial activities [3, 4].

Thousands of organic, inorganic and biological pollutants have been reported as water contaminants. Some of them have serious side effects and toxicities with a few being lethal and carcinogenic [5, 6]. These pollutants are very dangerous for all of us, aquatic conditions and the ecosystem of the earth as a whole. The United State National Primary Drinking Water Standards specify a maximum contaminant level (MCL) for a number of inorganic anions, including fluoride, nitrite, nitrate, chloride, phosphate and sulfate. Among such contaminants fluoride and phosphate are well known. Disposal of untreated waste containing fluoride and phosphate into water bodies may deteriorate water quality subsequently [7].

Contamination of fluoride in the ground and surface water could come either from natural geological sources including various minerals, such as fluorite, biotites, topazite and shale or from industries that uses fluoride containing compounds as raw materials, e.g., glass and ceramic production, semiconductor manufacturing, electroplating and aluminum smelters. In similar way industries such as fertilizer, semiconductor and phosphoric acid processing produce wastewater that contains high concentration of phosphate [8]. Excessive intake of these ions through food and

*Corresponding author. E-mail: endaleteju@yahoo.com

drinking water causes significant effect on the human body. Drinking of water from the ground water sources is the main route of fluoride intake in rural areas of underdeveloped countries.

According to the World Health Organization guidelines, the maximum concentration limit of fluoride is 1.5 mg/L for drinking water [9]. Concentrations higher than this not only affects teeth and skeleton but also cause several neurological damages in severe cases [10]. Phosphate can provide an additional nutrient for growth of photosynthetic macro and microorganisms in aquatic bodies, and also leads to eutrophication problem especially in enclosed water bodies [11]. Eutrophication can have considerable detrimental impacts on leisure or tourism, use of water, drinking water extraction, fish and other organisms. It results in the depletion of oxygen that leads to fish death and affects other aquatic life forms adversely [12]. Hence, it is necessary to use an effective and robust technique for the removal of excess fluoride and phosphate from water.

Various treatment procedures have been used for the removal of excess fluoride from water. Among them, adsorption, precipitation, coagulation, Donnan dialysis, electrodialysis, reverse osmosis, nanofiltration, electrolytic defluoridation and ultra-filtration are reported. Similarly, for phosphate removal various techniques including chemical precipitation, biological treatment, crystallization treatment, and methods such as electro coagulation, micro filtration, membrane bioreactors, nano filtration, reverse osmosis and adsorption have been used. Fluoride and phosphate can also be simultaneously removed by some novel methods, such as nanomagnetite aggregation process and hybrid precipitation–micro filtration process [8].

Among these potential separation technologies mentioned above, adsorption is one of the most promising methods because of its low initial cost, flexibility and simplicity of design and ease of operation and maintenance for removing contaminants from water. The efficiency of this technique mainly depends on the nature of the adsorbents [13] and on ions (adsorbate) in fluid diffusing to the surface of a solid (adsorbent), where they bond with the solid surface or are held there by weak intermolecular forces [14].

Depending on the types of interaction between adsorbate and adsorbent surface, chemisorptions and physical adsorption can be differentiated. Chemisorptions typically can show bonding energies above 200 kJ/mol. Here, the adsorbate reacts with the surface to form a covalent or an ionic bond. Physical adsorption on the other hand is a rapid process caused by nonspecific binding mechanisms such as van der Waals forces and results in bonding energies of 4-40 kJ/mol. Generally, physical adsorption is less specific for whichever compound adsorbed to surface sites, has weaker forces and energies of bonding, operates over longer distances (multiple layers), and is more reversible [15].

With regard to their application nanoparticles are of great scientific interest as they are effectively forming a bridge between bulk materials and atomic or molecular structures. Bulk materials have constant physical properties regardless of their size, but at the nano-scale size-dependent properties are often observed. There are several reasons for the great interest of the scientific community towards nanotechnology, but the primary motivation is because nanomaterials typically exhibit unique electronic, optical, and mechanical properties compared to their bulk counterpart and even molecular complements. Thus, nanomaterials have a number of key physico-chemical properties that they have a large surface area, enhanced reactivity, self-assembly and their wider availability make them particularly attractive separation media for water purification [16].

To the best of the authors' knowledge, there are no reports on removal of fluoride and phosphate from an aqueous solution by $Al_2O_3/Fe_3O_4/ZrO_2$ ternary mixed oxide nanosorbent. The wide variety of electronic and chemical properties of metal oxides makes them exciting materials for basic research and technological applications. Zirconium (IV) grafted Fe_3O_4 nanoparticles can be easily separated by an external magnetic field and simply recovered after washing with a basic aqueous solution [17]. It was also reported that Zr oxide and its mixed oxides have a high surface area [18]. This motivated us to work on adsorption of fluoride and phosphate from aqueous solution. Therefore, in this study nano sized $Al_2O_3/Fe_3O_4/ZrO_2$ ternary mixed oxide was

synthesized at the laboratory scale and used as an adsorbent to remove fluoride and phosphate from aqueous solutions. The synthesis process followed co-precipitation method due to its advantages including simple and rapid preparation, easy control of particle size and composition, homogeneity in mixed precipitates and high specific surface of the products [17]. The adsorption kinetics, adsorption isotherms, the effect of coexisting ions, thermodynamic parameters, desorption and applicability to real water samples were investigated. Additionally, the influence of operating parameters such as solution pH, the effect of ionic strength, contact time, adsorbent dose, initial adsorbate concentration and agitation speed were determined.

EXPERIMENTAL

Synthesis procedure of the adsorbents

$Al_2O_3/Fe_3O_4/ZrO_2$ ternary composite was prepared by co-precipitation of Fe:Al:Zr at a mole ratio of 70:25:5. In the first step, stoichiometrically calculated $FeCl_2.4H_2O$ and $FeCl_3.6H_2O$ (at 0.5 mole ratio of Fe^{2+}/Fe^{3+}) were dissolved in 100 mL of 0.3 M HCl solution. Then, the solution was added drop-wise from separatory funnel into the solution of 120 mL of 3 M NaOH (pH 12) over a period of 2 h, under a vigorous stirring at 80 °C in N_2 atmosphere to obtain Fe_3O_4 Ferro fluid. Following this, the magnetite–alumina–zirconia oxide composite was prepared by adding 100 mL of $Al(NO_3)_3.9H_2O$ and $ZrOCl_2.8H_2O$ (obtained by dissolving stoichiometric amounts of both salts in 100 mL of deionized water separately) into the obtained Fe_3O_4 suspension. The pH of the mixtures was adjusted to 8.0 using 0.1 M NaOH and the mixture was magnetically stirred under N_2 atmosphere for 1.5 h at 70 °C. Finally, the resulting black magnetic fluid was made to settle and washed with deionized water several times to remove impurities such as Cl^-, NO_3^- and excess OH^- ions and then dried at 60 °C for 24 h to obtain the desired product [19].

Elemental analysis

In this particular experiment, 0.1 g of the as-synthesized powder was digested with a mixture of acids to perform elemental analysis of Al, Fe, and Zr which was finally performed by flame atomic absorption spectrophotometer [20].

Characterization of the as-synthesized powder

The crystalline phases and the crystallite sizes of the as-synthesized nanosorbent before and after adsorption of fluoride and phosphate were determined using X-ray diffraction (XRD) instrument equipped with CuKα radiation (λ = 0.15405 nm). The surface functional groups of the nanocomposite before and after adsorption were determined by FTIR. Similarly, the specific surface area was investigated by Brunauer- Emmett-Teller (BET) technique.

Batch adsorption studies

Batch experiments were conducted using 250 mL Erlenmeyer flasks under continuous mixing conditions with magnetic stirrer at room temperature. The effect of different parameters such as dose of adsorbent, agitation speed, pH, ionic strength, contact time, initial concentration, and the presence of foreign ions were studied by varying one parameter at a time and keeping the others constant for both analytes in separate experiments. The residual F^-concentration was measured immediately using a fluoride selective electrode after an equal volume of TISAB was added on each sample solution. Then the potential response was converted to concentration by using the relation:

$$C_{F^-} = 10^{\frac{E-Const}{S}} \quad (1)$$

where C_F^- is the free fluoride concentration, E is the potential, S is the slope of the calibration curve and the constant is its y intercept [21]. On the other hand, final concentrations of the phosphate ions were determined spectrophotometrically by the molybdenum blue method by monitoring the absorbance at 880 nm on UV-Vis spectrophotometer [22]. Finally, removal efficiency was calculated by using the relationship in equations 2 and 3:

$$\% \text{ Adsorption} = \frac{(C_o - C_e)}{C_o} \times 100 \quad (2)$$

$$\text{Adsorption capacity} = \frac{(C_o - C_e)}{m} \times V \quad (3)$$

where C_o and C_e are initial and equilibrium concentrations of F^-/PO_4^{3-} (mg/L), respectively, m is quantity of the nanocomposite (g) and V is the volume required for the reaction mixture (L) [23].

Determination of the effect of ionic strength and pH study

The effect of pH on the adsorption of fluoride and phosphate was investigated by varying initial solution pH in the range 2-11 (2, 4, 5, 6, 7, 9 and 11) at room temperature. Here 0.1 g of the nanocomposite was mixed with 25 mL of 20 mg/L initial concentration of each analyte in separate flasks and agitated at a speed of 120 rpm for 24 h. Ionic strengths of 0.1 M, 0.01 M and 0.001 M $NaNO_3$ were chosen to investigate their effect on fluoride/phosphate adsorption by the nanocomposite. Determination of the pH of point of zero charge (pH_{PZC}) was also performed according to the procedure reported in [24].

The effect of adsorbent dose, contact time and agitation speed

The effect of adsorbent dose was investigated by mixing 25 mL of 20 mg/L of both analytes with different quantities of the nanocomposite ranging from 0.05-2 (0.05, 0.075, 0.1, 0.5, 1 and 2) g keeping other parameters constant in separate flasks. Similarly, the effect of contact time was also studied by varying time from 1- 48 (1, 4, 8, 12, 16, 24 and 48) h. The effect of agitation speed was also investigated by varying agitation speed from 50-200 (50, 100, 120, 150 and 200) rpm for both analytes. The pH of the solution was kept at optimized values [25].

The effect of concentration and coexisting ions

The effect of initial concentration was evaluated by varying it in the range of 10-140 (10, 20, 40, 60, 80, 100, 120, and 140) mg/L. On the other hand effect of coexisting ions on the adsorption of fluoride and phosphate ions on the as synthesized nanocomposite was also evaluated in the presences of 20 mg/L of SO_4^{-2}, NO_3^-, HCO_3^{-2} and Cl^-, respectively, and separately keeping other parameters (pH, adsorbent dose, contact time and agitation speed) constant at optimized values.

Adsorption isotherm, adsorption kinetics and thermodynamic study

Data for plotting isotherms were obtained by mixing initial concentrations ranging from 10-140 (10, 20, 40, 60, 80, 100, 120, and 140) mg/L and the optimized amount of adsorbent dose for both ions. Adsorption kinetics was studied by varying time ranging from 1, 4, 8, 12, 16 and 24 h and the nature and thermodynamic feasibility of the sorption process was determined by performing the adsorption process at 20, 30, 40, 50 and 60 ^oC. In all cases, the pre-optimized parameters were kept constant at their optimum values.

Desorption and recyclability study

To investigate desorption of fluoride/phosphate from the exhausted nanocomposite, the optimized adsorbent dose was subjected to adsorption for an optimized time in a 50 mL of initial concentration of fluoride/phosphate ion solution. Then the exhausted adsorbent was conditioned

(immersed) in 50 mL of 0.1 M NaOH solutions for desorption to take place by varying pH of the solution from 2-12. The recovery percentage was obtained from the following equations:

$$\text{Desorption efficency } \% = \frac{C_d - C_e}{C_o - C_e} \text{ x } 100 \quad (4)$$

where, C_d is desorbed concentration of fluoride/phosphate ion after the desorption process, C_e is equilibrium concentration and C_o is initial concentration of fluoride and phosphate [26]. To investigate the extent of regeneration and reusability of the adsorbents, experiments were performed at pre optimized conditions and desorption was done by using 0.1M NaOH up to four cycles. Then the % adsorption of fluoride/phosphate on the adsorbent for each cycle was recorded [27].

Applicability on real water samples treatment

To assess the applicability of the method on real samples, ground water was taken from Adama Town on March 5, 2016 and lake water from Lake Adele on March 19, 2016 (Haramaya Woreda, Ethiopia) for fluoride and phosphate study, respectively. First, the initial concentration of fluoride and phosphate in these water samples were determined before loading the adsorbent. Then the synthesized nanosorbent was mixed with 50 mL of these water samples at the optimized condition to see its removal capacity.

RESULTS AND DISCUSSION

Powder X-ray diffraction analysis

Adsorption reaction may lead to changes in the molecular and crystalline structure of the adsorbent and hence understanding of these properties and the resulting changes thereof would provide valuable information regarding adsorption reaction [28]. Hence XRD patterns of the adsorbent before and after treatment with fluoride and phosphate ions were studied and presented in Figure 1.

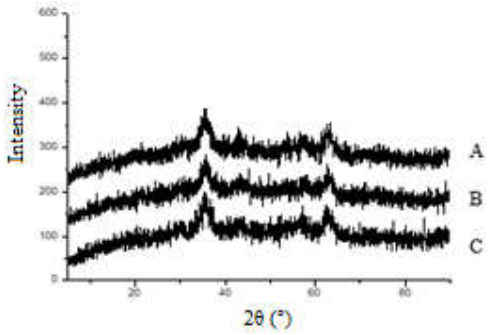

Figure 1. XRD pattern of $Al_2O_3/Fe_3O_4/ZrO_2$ mixed oxide (A = before adsorption, B = after PO_4^{3-} adsorption and C = after F^- adsorption).

As shown in Figure 1, the XRD pattern of $Fe_3O_4/Al_2O_3/ZrO_2$ nanocomposite before and after adsorption exhibited no variation in the structure and this suggested that the fluoride and phosphate ions might diffuse into micropores and macropores without altering the structure of the adsorbent. A similar phenomenon was observed in the sorption study of phosphate by Fe-Al-Mn mixed oxide [29]. The diffraction pattern shows very weak intensities on a broad background

suggesting the amorphous nature of the adsorbent. However, the presence of some low intensity peaks at 2θ values of 35.25, 43.42, 53.69, 57.46 and 63.33° could be attributed to a face centered cubic spinel structure of magnetite (Fe_3O_4) [19].

FTIR analysis

The FTIR spectra of $Al_2O_3/Fe_3O_4/ZrO_2$ ternary oxide before and after adsorption of fluoride and phosphate are presented in Figure 2.

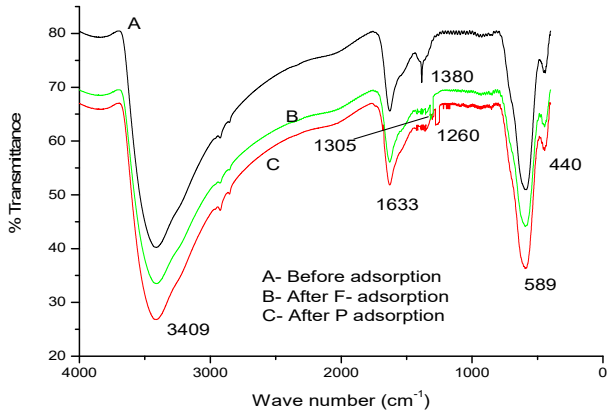

Figure 2. FT-IR spectra of the as-synthesized nanosorbent (A = before adsorption, B = after F^- adsorption and C = after PO_4^{3-} adsorption).

The strong and broad band at 3600–3100 cm^{-1} region (O-H stretching vibration) may be assigned for the presence of hydroxyl of coordinated water molecules [30]. The band at 1633 cm^{-1} primarily attributed to the bending vibration of H-O-H (physisorbed water molecules) [29]. When comparing the spectrum of $Al_2O_3/Fe_3O_4/ZrO_2$ ternary oxide before adsorption with the spectrum after adsorption, the peak at 1380 cm^{-1} (surface hydroxyl group, M-OH) before adsorption was weakened dramatically and this was accompanied by the formation of new peaks observed at 1305 cm^{-1} and 1260 cm^{-1} after adsorption of fluoride and phosphate, respectively. These results approved that fluoride and phosphate were successfully adsorbed on the surface of $Al_2O_3/Fe_3O_4/ZrO_2$ ternary oxide [30]. The peak appearing at 1260 cm^{-1} in the spectrum after adsorption was attributed to the bending vibration of adsorbed phosphate. This indicates that replacement of surface hydroxyl groups (M-OH) by phosphate via the formation of inner sphere complex [29]. The spectral peak obtained at 1305 cm^{-1} may signify the adsorption of fluoride on the adsorbent possibly through electrostatic attraction. The bands at 589 cm^{-1} and 440 cm^{-1} may be assigned to M-O symmetrical stretching vibrations of the mixed metal oxides [31].

Surface area

The specific surface area of the as-synthesized adsorbent was determined by Brunauer–Emmett–Teller (BET) N_2 adsorption and desorption isotherms. This study provided the specific surface area of $Al_2O_3/Fe_3O_4/ZrO_2$ ternary oxide which was found to be 205 m^2/g. The high specific surface area may have resulted from the presence of zirconium (ZrO_2) oxides [32]. Therefore, $Al_2O_3/Fe_3O_4/ZrO_2$ ternary oxide can be categorized as adsorbent with high adsorption capacity.

Elemental analysis

Analysis of the synthesized nanocomposite by flame atomic absorption spectrometer indicated that the percentage compositions of Fe, Al and Zr in the as-synthesized nanocomposite were found to be 72.3%, 23.9% and 3.8%, respectively. These percentage compositions are close to the ratio of each metal ion (70:25:5) taken during the synthesis process.

pH of point of zero charge

The pH of point of zero charge of the $Al_2O_3/Fe_3O_4/ZrO_2$ nanocomposite was found to be 5.71 as presented on Figure 3a. Thus, the adsorption of phosphate and fluoride on the adsorbent is favored at pH below 5.71.

The effect of ionic strength

Ionic strength is an important parameter especially when solute removal is affected by slight changes in the supporting electrolyte solution [33]. Table 1 shows the % removal and adsorption capacity of phosphate and fluoride in the presence of $NaNO_3$.

Table 1. Percentage removal and adsorption capacity of $Al_2O_3/Fe_3O_4/ZrO_2$ in the presence of $NaNO_3$.

$NaNO_3$ conc. (M)	Fluoride			Phosphate		
	C_e (mg/L)	q_e (mg/g)	% Ads	C_e (mg/L)	q_e (mg/g)	% Ads
0.1	3.18±0.364	0.840	84.12	0.075±0.009	2.481	99.25
0.01	2.64±0.110	0.868	86.80	0.051±0.010	2.487	99.49
0.001	2.15±0.155	0.893	89.25	0.037±0.006	2.490	99.60

The result indicates that the percentage removal of fluoride onto $Al_2O_3/Fe_3O_4/ZrO_2$ decreased as concentration of $NaNO_3$ increased under the concentration range studied. High $NaNO_3$ concentration indicates more NO_3^- ions existing on the outer layer which would exert a strong repulsive force against the approaching F^- ion leading to a decrease in the adsorption capacity of $Al_2O_3/Fe_3O_4/ZrO_2$. On the other hand, no significant change was observed on phosphate adsorption as concentration of $NaNO_3$ increased from 0.001 to 0.1 M [33]. Therefore, from the results it can be inferred that outer sphere complexation could be formed when fluoride was adsorbed on $Al_2O_3/Fe_3O_4/ZrO_2$ as removal capacity depends on concentration of $NaNO_3$. On the other hand, PO_4^{3-} adsorption was through the formation of inner sphere complexes since concentration of $NaNO_3$ has no significant change on its percentage removal.

Optimization of experimental parameters

Batch mode of adsorption was used to optimize experimental parameters, including solution pH, adsorbent dose, speed of agitation, contact time and initial fluoride and phosphate ions concentration. The optimum value for each parameter was found to be 4, 0.5 g, 100 rpm, 12 h and 20 mg/L for fluoride and 5, 0.1 g, 100 rpm, 8 h and 10 mg/L for phosphate.

The adsorption of fluoride onto the as-synthesized adsorbent increased as pH increased from 2 to 4 (90 to 92.93%) (Figure 3b). A similar trend was observed on phosphate adsorption up to pH 5 (increased from 72.75 to 96.63%). Thus, maximum adsorption for fluoride and phosphate was achieved at pH 4 and 5, respectively. The decrease in the sorption capacity at higher pH can be attributed to the competition for the active site by OH^- ions and or the development of negative charge on the adsorbent surface, since both OH^- ions and F^-/PO_4^{3-} ions have the same charge [34, 35].

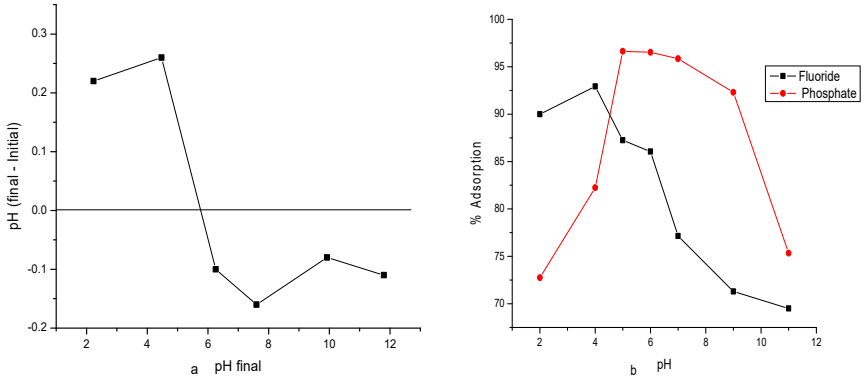

Figure 3. Plots of (a) pH of point zero charge and (b) the effect of pH on fluoride and phosphate adsorption onto Al_2O_3/Fe_3O_4 /ZrO_2 (at dose 0.1 g, initial concentration 20 mg/L and contact time of 24 h).

Adsorption isotherm study

The relationship between the amount of substance adsorbed at constant temperature and its concentration in the equilibrium solution is called the adsorption isotherm [36]. The most widely accepted surface adsorption models for single-solute systems (Langmuir and Freundlich) were selected in this study [37].

The Freundlich isotherm in its linear form is represented by:

$$\text{Log } q_e = \log K_f + \frac{1}{n \log C_e} \quad (5)$$

$$q_e = K_f C_e^{1/n} \quad (6)$$

where, q_e is the amount of solute adsorbed per unit weight of the sorbent (mg/g), C_e is the equilibrium concentration of solute in solution (mg/L), K_f is a measure of adsorption capacity and 1/n is the adsorption intensity. The Freundlich isotherm constants 1/n and K_f can be calculated from the slope and intercept of the plot logq_e vs logC_e. The values of 1/n lying between 0 and 1 and the *n* values lying between 1 and 10 indicate favorable conditions for adsorption. The intercept of the line, K_f, is roughly indicator of the adsorption capacity [38]. On the other hand, the Langmuir equation is useful for the estimation of maximum adsorption capacity corresponding to complete monolayer coverage and expressed by:

$$q_e = \frac{Q_o b C_e}{1 + b C_e} \quad (7)$$

The linearized form of equation 7 is given in equation 8:

$$\frac{C_e}{q_e} = \frac{1}{Q_o \text{b}} + \frac{C_e}{Q_o} \quad (8)$$

where, Q_o is the amount of adsorbate at complete monolayer coverage (mg/g) and gives the maximum sorption capacity of sorbent, C_e is the equilibrium concentration of fluoride/phosphate (mg/L) and b (L/mg) is the Langmuir isotherm constant that relates to the energy of adsorption. Langmuir constants Q_o and b can be calculated from the slope and intercept of the plot C_e/q_e versus C_e, respectively. The plot C_e/q_e vs C_e yields a straight line with a slope $1/Q_o$ and an intercept $1/Q_o$b. The values of all parameters of the two models are given in Table 2.

Table 2. Langmuir and Freundlich isotherm values for fluoride and phosphate adsorption onto $Al_2O_3/Fe_3O_4/ZrO_2$ ternary nanocomposite.

Analyte	Langmuir				Freundlich		
	Q_o (mg/g)	B	R_L	R^2	K_f	1/n	R^2
Fluoride	8.97	0.113	0.31	0.9091	0.973	0.679	0.9478
Phosphate	33.33	1.035	0.089	0.9686	13.24	0.427	0.9465

The feasibility of the isotherm can be tested by calculating the dimensionless constant, R_L expressed as:

$$R_L = \frac{1}{1+bC_o} \quad (9)$$

The value of R_L indicates the type of isotherm: to be irreversible if ($R_L = 0$), favorable if ($0 < R_L < 1$), linear if ($R_L = 1$), or unfavorable for ($R_L > 1$) [38]. Thus, the calculated values of R_L for phosphate and fluoride adsorption onto Al-Fe-Zr ternary oxide were found to be between 0 and 1 indicating the favorability of the adsorption process.

Langmuir's and Freundlich's curves were interpreted with respect to correlation coefficient R^2, a statistical measure of how well the regression line approximates the real data point. An R^2 value of 1.0 indicates that the regression line perfectly fits the data. In this study, the R^2 values of the nano sized adsorbent in Freundlich's equation exhibits a higher value than Langmuir's (i.e. 0.9478 and 0.9091, respectively) in the case of fluoride, whereas phosphate adsorption indicates a higher R^2 value in Langmuir plot than Freundlich plot (0.9686 and 0.9465, respectively). Therefore, fluoride and phosphate adsorption onto the nanosized adsorbent best fits with Freundlich and Langmuir equation respectively. The Freundlich and Langmuir equation for the fluoride adsorption process has been developed as indicated in the equation (10) and (11), respectively.

$$q_e = 0.973C_e^{0.679} \quad (10)$$

$$q_e = 1.01361C_e/1+0.113C_e \quad (11)$$

Similarly, the Freundlich and Langmuir equations for the phosphate adsorption process are indicated in the equation (12) and (13), respectively.

$$q_e = 13.24C_e^{0.427} \quad (12)$$

$$q_e = 34.5C_e/1+1.035C_e \quad (13)$$

Adsorption kinetics

The adsorption kinetics of the synthesized nanosorbent for the two analytes was studied by varying contact time from 1 to 24 h. In this study the Lagergren pseudo-first and pseudo-second order models were considered. The pseudo-first order adsorption kinetics model is given in equation 14.

$$\log(q_e - q_t) = \log q_e - \frac{k_1}{2.303}t \quad (14)$$

where, q_e and q_t are the amount of fluoride/ phosphate adsorbed (mg/g) at equilibrium and at any time t (min), respectively. The adsorption rate constant, k_1 was determined from the slope of the linear plot of $\log(q_e - q_t)$ versus t (i.e., $k_1 = -2.303 \times$ slope) and q_e is obtained from intercept ($\log q_e$ = intercept). On the other hand, the integrated form at boundary conditions (t = 0 to t = t) and ($q_t = 0$ to $q_t = q_t$) for the pseudo-second order adsorption kinetic model is expressed as:

$$\frac{1}{q_e - q_t} = \frac{1}{q_e} + k_2\, t \quad (15)$$

$$\frac{t}{q_t} = \frac{1}{k_2 q_e 2} + \frac{1}{q_e} t \quad (16)$$

where, q_t and q_e are the amounts of adsorbed analyte at a time t and equilibrium (mg/g), respectively, k_2 is the rate constant (g mg^{-1} min^{-1}), t is the stirring time (min), k_2 which is ($slope^2$/intercept) can be determined from plotting t/q_t against t based on the above equation and the value of q_e is 1/slope. The Lagergren pseudo-first and pseudo-second order reactions were interpreted with respect to coefficient of determination, R^2, and by comparing the calculated q_e value with the corresponding experimental q_e value. Thus, the result in Table 3 indicates that the adsorptions of fluoride and phosphate onto $Al_2O_3/Fe_3O_4/ZrO_2$ follow second order reaction.

Table 3. The values of parameters and coefficient of determination of kinetic models for fluoride and phosphate adsorption onto $Al_2O_3/Fe_3O_4/ZrO_2$ nanocomposite.

Analyte	C_o (mg/L)	q_e (mg/g) experimental	Pseudo-first order			Pseudo-second order		
			q_e (mg/g) calc.	K_1	R^2	q_e (mg/g) calc.	K_2	R^2
F^-	20	0.933	0.75	0.050	0.636	0.935	10.60	1
PO_4^{3-}	10	2.470	3.76	0.047	0.613	2.501	18.43	1

Adsorption thermodynamics study

The standard free energy change (ΔG), enthalpy change (ΔH) and entropy change (ΔS) are the main thermodynamic characteristics of any adsorption system in equilibrium. The fundamental thermodynamic equation that relates all the above three parameters is given in equation 17 [39].

$$\Delta G = \Delta H - T\Delta S \quad (17)$$

where ΔG is in kJ/mol, ΔH is in kJ mol^{-1}, ΔS is in kJ $mol^{-1}K^{-1}$ and T is in K. The free energy of adsorption, considering the adsorption equilibrium constant K is given by equation 18:

$$\Delta G = -RT \ln K_c \quad (18)$$

where, R is the universal gas constant (8.314 J $mol^{-1}K^{-1}$) and K_c is the equilibrium constant obtained from q_e/C_e. ΔH and ΔS can be determined from the plot of $\ln K_c$ versus T^{-1} by computing their slope and intercept (i.e. ΔH = -slope × R and ΔS = intercept × R). From equations (17) and (18) a relationship between lnK and T can be derived and is indicated in equation 19. The calculated thermodynamic parameters for the adsorption process of fluorine and phosphate onto the adsorbent are as shown in Table 4.

$$\ln K_c = \Delta S/R - \Delta H/TR \quad (19)$$

The positive values of ΔG in fluoride adsorption study confirms that the adsorption process is non spontaneous. The value of ΔH was positive, indicating that the adsorption reaction was endothermic. So, increasing temperature encourages fluoride ion adsorption. Enhancement of adsorption capacity of $Al_2O_3/Fe_3O_4/ZrO_2$ at higher temperature may be attributed to the enlargement of the pore size and/or activation of the adsorbent surface and also increase in the mobility of fluoride ions. The positive value of ΔS reflects high degrees of disorderliness at the solid solution interface during the adsorption of fluoride onto $Al_2O_3/Fe_3O_4/ZrO_2$. This may be due to the fact that the adsorbed water molecules which are displaced by the adsorbate species, gain more translational entropy than it is lost by the adsorbate molecules, thus allowing the prevalence of randomness in the system [28]. In case of the phosphate adsorption process, the negative values of ΔG confirm that the adsorption process is spontaneous, which becomes a less negative value with an increase in temperature, indicating that adsorption occurred at a lower temperature. The negative values of enthalpy confirm that the exothermic nature of the adsorptions process and

-40.32 (kJ/mol) amount of heat was released during the binding of phosphate on the surface of Al/Fe/Zr mixed oxide. The negative value of entropy indicates decreasing randomness at solid-liquid interface during adsorption.

Table 4. Calculated thermodynamic constants of the fluoride and Phosphate adsorption onto $Al_2O_3/Fe_3O_4/ZrO_2$ mixed oxide.

Analyte	Temp (K)	ln K_c	ΔG (kJ/mol)	ΔH (kJ/mol)	ΔS (J/molK)
Fluoride	293	-1.394	3.396	16.744	45.9
	303	-1.06	2.670		
	313	-0.879	2.287		
	323	-0.742	1.268		
	333	-0.546	1.512		
Phosphate	293	3.974	-9.681	-40.323	-106.3
	303	3.21	-8.086		
	313	2.53	-6.584		
	323	2.12	-5.693		
	333	1.96	-5.426		

The effect of coexisting ions study

In the present study we investigated the possibility of interference by HCO_3^-, Cl^-, NO_3^- and SO_4^{2-} on fluoride and phosphate removal. The results in Figure 4 indicates that the percentage removal in the presence of these ions ranged from 72.65 - 84% for fluoride and 95.5 - 99.3% for phosphate. Fluoride adsorption is more affected in the presence of sulphate and phosphate due to their competion for the active sites as they are all negatvely charged [11]. Bicarbonate and nitrate have less effect on its adsorption whereas phosphate adsorption was more affected in the presence of nitrate and fluoride when compared with the other ions.

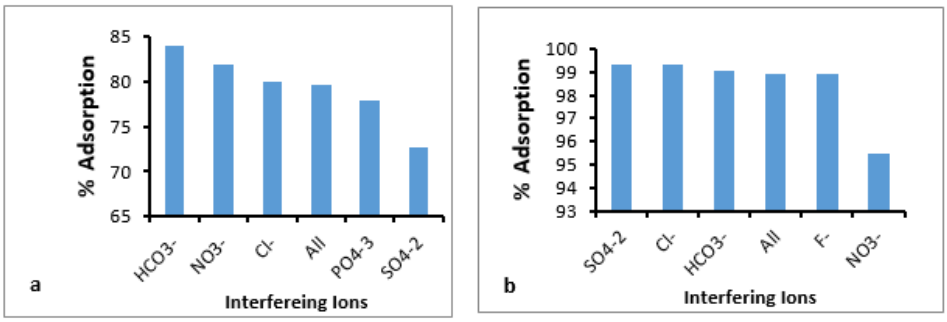

Figure 4. The effect of coexisting ions (a) on fluoride adsorption (pH 4, dose 0.5 g, C_o 20 mg/L) and (b) on phosphate adsorption (pH 5, dose 0.1 g, C_o 20 mg/L) at speed of 100 rpm.

Desorption study

Ions desorbability can be defined as the ratio of the desorbed ions over the total adsorbed ions by the adsorbent. Therefore, the desorbability can be used to indicate the degree of fluoride/phosphate desorption from the adsorbent [40]. In this particular experiment, pH of the solution was varied from 2-12 (2, 4, 5, 6, 8, 10 and 12) to observe the effect of solution pH on desorption of fluoride and phosphate from the nanosized adsorbent. Desorption of fluoride increased from 3.31 to 77.7% while that of phosphate from 0.25 to 85% when pH of the solution

was increased from 2 to 12. These results indicated that desorption was more favorable at higher pH for both ions. Up to pH 8 desorption of both ions took place slightly, then increased abruptly. When compared to fluoride, desorption of phosphate was more difficult at low pH. The maximum desorption was obtained at pH 12 (77.7 and 85.1%) for fluoride and phosphate, respectively, which is in agreement to the inner sphere adsorption mechanism of the two ions on the sorbent material [41].

Recyclability study

To make a cost effective and user-friendly process, the adsorbent should be regenerated, so as to reuse for further fluoride and phosphate adsorption. In this study the experiments were performed using optimized conditions and desorption was done by using 0.1 M NaOH up to four cycles. As presented in Table 5, the percentage removal of fluoride and phosphate was found to be promising up to the fourth cycle.

Table 5. The recyclability study of the synthesized nanosorbent for fluoride and phosphate sorption.

Analyte	Cycle 0	Cycle 1	Cycle 2	Cycle 3	Cycle 4
	% Removal	% Removal	% Removal	% Removal	% Removal
Fluoride	93.75	89.5	85.5	78.25	73
Phosphate	99.33	98.86	96.24	93.1	90.2

Applicability on real water samples treatment

To assess the applicability of the method for real samples, ground water was taken from Adama town for fluoride and lake water from Lake Adele (Haramaya Woreda) for phosphate adsorption study. The initial concentrations of fluoride and phosphate in these water samples were determined before loading the adsorbent. Then the water samples were mixed with the adsorbent by both batch and column methods and the result are presented in Table 6. In column method, the sample solution was passed through the column at a flow rate of 5 mL/min.

Table 6. Applicability of the nanosorbent on the real water samples (n = 3).

Analyte	Initial conc. (mg/L) in water samples	Concentration (mg/L) after loading the adsorbent			
		Batch method	Column method		
			Cycle 1	Cycle 2	Cycle 3
Fluoride	4.92±0.383	1.97±0.192	2.57±0.225	2.033±0.116	1.362±0.11
Phosphate	1.7±0.32	0.35±0.048	0.33±0.09	0.265±0.102	0.077±0.032

Results of the batch method show that the fluoride content of the ground water was decreased to 1.97 mg/L from 4.92 mg/L and the phosphate content of the lake water decreased to 0.35 mg/L from 1.7 mg/L. The fluoride content was decreased to maximum permissible level after passing through the column packed with the adsorbent for three times (i.e., below 1.5 mg/L).

CONCLUSION

The findings of the present study indicate that fluoride and phosphate uptakes from the water by $Al_2O_3/Fe_3O_4/ZrO_2$ were found to be dependent on the pH, contact time, initial fluoride and phosphate concentration, adsorbent dose and temperature. The results of the study also revealed that the synthesized nanosorbent has high removal capacity of phosphate than fluoride. $Al_2O_3/Fe_3O_4/ZrO_2$ oxide is amorphous at the synthesized temperature since no strong crystal

structure peak was observed and it has a high specific surface area (205 m^2/g) as indicated by XRD and BET study, respectively. The adsorption isotherms of fluoride better fitted to Freundlich model whereas that of phosphate better fitted to Langmuir model. The adsorption kinetics data indicated that the adsorption of both ions on the synthesized nanosorbent follows pseudo-second order reaction. The adsorption of fluoride was found to be non-spontaneous and endothermic whereas that of phosphate was spontaneous and exothermic. Results from this study demonstrated potential utility of tested $Al_2O_3/Fe_3O_4/ZrO_2$ as a viable technology for fluoride and phosphate removal from drinking water.

ACKNOWLEDGMENTS

The authors would like to acknowledge the financial support received from the Ministry of Education through the School of Graduate Studies, Haramaya University. The support in characterizing our samples received from Instituto de Catalisis y Petroleoquimica, CSIC, is highly appreciated. The financial support obtained from Haramaya University via project codes (HURG-2016-03-02 and HURG-2020–03-02–75) is also duly acknowledged.

REFERENCES

1. Okello, C.; Tomasello, B.; Greggio, N.; Wambiji, N.; Antonellini, M. Impact of population growth and climate change on the freshwater resources of Lamu Island, Kenya. *Water* **2015**, 7, 1264-1290.
2. Camara, M.; Jamil, N.R.; Abdullah, A.F.B. Impact of land uses on water quality in Malaysia: a review. *Ecol. Process* **2019**, 8, 1-10.
3. Bhateria, R.; Jain, D. Water quality assessment of lake water: a review. *Sustain. Water Resour. Manag.* **2016**, 2, 161–173.
4. Dunca, A.M. Water pollution and water quality assessment of major transboundary rivers from Banat (Romania). *J. Chem.* **2018**, 1-8. https://doi.org/10.1155/2018/9073763.
5. Sharma, S.; Bhattacharya, A. Drinking water contamination and treatment techniques. *Appl. Water Sci.* **2017**, 7, 1043–1067.
6. Srinivasan, R. Advances in application of natural clay and its composites in removal of biological, organic, and inorganic contaminants from drinking water. *Adv. Mater. Sci. Eng.* **2011**, 1-18. doi:10.1155/2011/872531
7. Lu, N.C.; Liu, J.C. Removal of phosphate and fluoride from waste water by a hybrid precipitation–microfiltration process. *Sep. Purif. Technol.* **2010**, 74, 329–335.
8. Cai, P.; Zheng, H.; Wang, C.; Man, H.W. Competitive adsorption characteristic of fluoride and phosphate on Calcined Mg-Al-CO_3 layered double hydroxides. *J. Hazard. Mater.* **2012**, 213, 100-108.
9. World Health Organization (WHO). *Guidelines for Drinking Water Quality*: *World Health Organization*, Geneva; **199**3; pp. 45–46.
10. Kagne, S.; Jagtap, S.; Dhawade, P.; Kamble, S.P.; Devotta, S.; Rayalu, S.S. Hydrated cement: A promising adsorbent for the removal of fluoride from aqueous solution. *J. Hazard. Mater.* **2008**, 154, 88-95.
11. Liu, R.; Guo, J.; Tang, H. Adsorption of fluoride, phosphate and arsenate ions on a new type of ion exchange fiber. *J. Colloid Interface Sci.* **2002**, 248, 268-274.
12. Das, J.; Patra, B.S.; Baliarsingh, N.; Parida, K.M. Adsorption of phosphate by layered double hydroxides in aqueous solutions. *Appl. Clay Sci.* **2006**, 32, 252-260.
13. Bhatnagar, A.; Kumar, E.; Sillanpaa, M. Fluoride removal from water by adsorption. *Chem. Eng. J.* **2011**, 171, 811-840.

14. Li, Y.; Zhang, P.; Du, Q.; Peng, X.; Liu, T.; Wang, Z.; Xia, Y.; Zhang, W.; Wang, K.; Zhu, H.; Wu, D. Adsorption of fluoride from aqueous solution by graphene. *J. Colloid Interface Sci.* **2011**, 363, 348-354.
15. Zhang, P.; Chen, Y.P.; Wang, W.; Shen, Y.; Guo, J.S. Surface plasmon resonance for water pollutant detection and water process analysis. *Trends Anal. Chem*. **2016**, 85, Part C, 153-165.
16. Patel, G.; Pal, S.; Menon. Removal of fluoride from aqueous solutions by CaO nanoparticles. *Sep. Sci. Technol.* **2009**, 44, 2806-2826.
17. Poursaberi, T.; Hassanisadi, M.; Torkestani, K.; Zare, M. Development of zirconium(IV)-metalloporphyrin grafted Fe_3O_4 nanoparticles for efficient fluoride removal. *Chem. Eng. J.* **2012**, 1, 189–190.
18. Fahmida, G.; Yoshikazu, K.; Akira, N.; Kiyoshi, O. Preparation of alumina–iron oxide compounds by gel evaporation method and its simultaneous uptake properties for $Ni_2^+NH_4^+$ and $H_2PO_4^-$. *J. Hazard. Mater.* **2009**, 169, 697–702.
19. Kassahun, F. Synthesis and characterization of $Al_2O_3/Fe_3O_4/ZrO_2$ hetero junction ternary oxides nanocomposite for nitrate sorption from aqueous solution. M.Sc. Thesis, Haramaya University, Haramaya, Ethiopia, **2015**.
20. Abebe, B.; Taddesse, A.M.; Kebede, T.; Teju E.; Diaz, I. Fe-Al-Mn ternary oxide nanosorbent: Synthesis, characterization and phosphate sorption property. *J. Environ. Chem. Eng.* **2017**, 5, 1330–1340.
21. Workneh, G. Synthesize and characterize nano sized ternary Al-Fe-Mn mixed oxide sorbent for fluoride removal from aqueous solution. M.Sc. Thesis, Haramaya University, Haramaya, Ethiopia, **2013**.
22. Pradhan, S.; Pokhrel, M.R. Spectrophotometric determination of phosphate in sugarcane juice, fertilizer, detergent and water samples by molybdenum blue method. *Sci. World* **2013**, 11, 58-62.
23. Jung, K.W.; Hwang, M.J.; Ahn, K.H.; Ok, Y.S. Kinetic study on phosphate removal from aqueous solution by biochar derived from peanut shell as renewable adsorptive media. *Int. J. Environ. Sci. Technol.* **2015** 12:3363–3372.
24. Panumati, S.; Chudecha, K.; Vankhaew, P. Adsorption of phenol from diluted aqueous solutions by activated carbons obtained from bagasse, oil palm shell and pericarp of rubber fruit. *J. Sci. Technol.* **2008**, 30, 185-189.
25. Ahmed, T.S.; Taddesse, A.M.; Kebede, T.T. Synthesis, characterization and analytical evaluation of nano-sized iron/aluminum mixed oxide sorbent system for removal of phosphate from aqueous system. *J. Environ. Chem. Eng.* **2016**, 2458-2468.
26. Liu, W.; Wang, T.; Alistair, G.L.B.; Wang, Y.; Yin, X.; Li, X.; Ni, J. Adsorption of Pb^{2+}, Cd^{2+}, Cu^{2+} and Cr^{3+} onto titanate nanotubes: Competition and effect of inorganic ions. *Sci. Total Environ.* **2013**, 456, 171-180.
27. Raka, M.; Sirshendu, D. Adsorptive removal of nitrate from aqueous solution by polyacrylonitrile–alumina nanoparticle mixed matrix hollow-fiber membrane. *J. Membr. Sci.* **2014**, 466, 281– 292.
28. Arravinda, V.; Elango, K.P. Adsorption of fluoride on to magnesia. *Indian J. Chem. Technol.* **2006**, 13, 476-483.
29. ianbo, L.; Huijuan, L.; Zaho, X.; Liping, S.; Jihu, Q. Adsorptive removal of phosphate by a nanostructured Fe-Al-Mn trimetal oxide sorbent. *Powder Technol.* **2013**, 233, 146-154.
30. Long, F.; Gong, J.L.; Zeng, G.M.; Chen, L. Removal of phosphate from aqueous solution by magnetic Fe-Zr binary oxide. *J. Chem. Eng.* **2011**, 171, 448-455.
31. Zhang, G.S.; Liu, H.J.; Liu, R.P.; Qu, J.H. Removal of phosphate from water by a Fe–Mn binary oxide adsorbent. *J. Colloid Interface Sci.* **2009**, 335, 168-174.
32. Fahmida, G.; Yoshikazu, K.; Akira, N.; Kiyoshi, O. Preparation of alumina–iron oxide compounds by gel evaporation method and its simultaneous uptake properties for $Ni_2^+NH_4^+$ and $H_2PO_4^-$. *J. Hazard. Mater.* **2009**, 169, 697-702.

33. Futalan, C.M.; Tsai, W.C.; Lin, S.S.; Dalida, M.L.; Wan, M.W. Copper, nickel and lead adsorption from aqueous solution using chitosan-immobilized on bentonite in a ternary system. *Sustainable Env. Res.* **2012**, 22, 345-355.
34. Shemelis, B.; Zewge, F; Chandravanshi, B.S. Removal of excess fluoride from water by aluminium hydroxide. *Bull. Chem. Soc. Ethiop.* **2006**, 20, 17-34.
35. Almanassra, I.W.; Mckay, G.; Kochkodan, V.; Atieh, M.A.; Al-Ansari, T. A state of the art review on phosphate removal from water by biochars. *Chem. Eng. J.* **2021**, 409, 128211.
36. Karthikeyan, G.; Ilango, S. Fluoride sorption using *Morringa indica* based activated carbon. *J. Environ. Health Sci. Eng.* **2007**, 4, 21-28.
37. Kumar, E.; Bhatnagar, A.; Kumar, U.; Sillanpaa, M. Defluoridation from aqueous solution by nano–alumina: Characterization and Sorption studies. *J. Hazard. Mater.* **2011**, 186, 1042-1049.
38. Ayawei, N.; Ebelegi, A.N.; Wankasi, D. Modelling and interpretation of adsorption isotherms. *J. Chem.* **2017**, 1-11.
39. Rodrigues, L.A.; Silva, M.C.P. An investigation of phosphate adsorption from aqueous solution onto hydrous niobium oxide prepared by co-precipitation method. *Colloids Surf. A* **2009**, 334, 191-196.
40. Zeng, L.; Li, X. M.; Liu, J. Adsorptive removal of phosphorus from aqueous solution using iron oxide tailings. *Water Res.* **2004**, 38, 1318-1326.
41. Strawn, D.G. Sorption Mechanisms of Chemicals in Soils. A review. *Soil Syst.* **2021**, 5, 13, 1-22. https://doi.org/10.3390/soilsystems5010013.